R. JASIONOWSKI, W. POLKOWSKI, D. ZASADA

ISSN 0543-5846
METABK 56(1-2) 67-70 (2017)
UDC – UDK 669.15-621.746.7:539.21:620.18:66.014=111

RELATIONSHIP BETWEEN CRYSTALLOGRAPHIC TEXTURE AND CAVITATION RESISTANCE OF AS-CAST X8CrNi25-21 AND X6CrAl13 STEELS

Received – Primljeno: 2016-06-21
Accepted – Prihvaćeno: 2016-09-25
Original Scientific Paper – Izvorni znanstveni rad

In this paper, results of the cavitation resistance evaluation of as-cast X8CrNi25-21 austenitic steel and X6CrAl13 ferritic steel having a various grain orientations, are shown. It was found that the austenitic steel with a preferred < 110 >// ND orientation (where ND is a normal direction to the surface that was exposed to the cavitation process) exhibits a superior cavitation resistance over other examinated materials.

Key words: cast alloy steels, chemical composition, cavitation, crystallographic texture

INTRODUCTION

Metals and alloys are important group of structural materials that are applied in all branches of industry and engineering. Most of them crystallize in the face centered cubic (fcc), the body centered cubic (bcc) or the hexagonal close packed (hcp) crystal lattice type. Depending on the crystal structure, metallic materials exhibit various mechanical behaviors related to the activation of deformation mechanisms, namely a dislocation slip or a mechanical twinning [1-3].

The crystallographic structure has also a strong impact on a course of cavitation damage in liquid flowing installations. In these devices, a cavitation phenomenon takes place, i.e. the formation and growth of bubbles filled with a steam or dissolved gases in a reduced pressure areas of liquid, followed by their rapid decay (an implosion) in areas with an elevated pressure. The presence of gas inside the bubbles allows their reconstitution after the implosion, thus this process can be repeated several times [4,5].

In this paper, the effect of texture on the cavitation resistance of as-cast X8CrNi25-21 austenitic steel (fcc) and X6CrAl13 ferritic steel (bcc), was analyzed.

EXPERIMENTAL RESEARCH

The cavitation resistance was evaluated on two investigated materials: X8CrNi25-21 austenitic steel and X6CrAl13 ferritic steel. Both steel were melted and casted in a vacuum induction furnace that gives proper conditions to receive predesigned chemical compositions of alloys (in a narrow content range of particular elements) and a high metallurgical quality. Chemical compositions of investigated steels are listed in Table 1.

Table 1 **Chemical composition of X8CrNi25-21 and X6CrAl13 steels / mas. %**

Element	Steel	
	X8CrNi25-21	X6CrAl13
C	0,08	0,06
Cr	25,0	13,0
Ni	21,0	-
Al	0,20	0,20
Si	1,50	1,00
Mn	2,00	1,00
Fe	Bal.	Bal.

The investigated steels in as cast states were characterized by different hardness values, i.e. 219 and 171 HV for X8CrNi25-21 austenitic steel and X6CrAl13 ferritic steel, respectively.

The fabricated castings had cylindrical shape with a height of 180 mm and a diameter of 60 mm.

Both steels in as cast states were characterized by a very large grain size (the equivalent grain diameter was even up to 6 mm). Two types of samples were used upon the cavitation experiment: one that was cut off perpendicular to the casting axis and the second that was cut off parallel to the casting axis the casting axis and the second that was cut off parallel to the casting axis.

It was found that in the case of X8CrNi25-21 austenitic steel the former sample exhibits the < 110 >// ND texture (Figure 1a,b), while the later posses the < 100 >// ND texture (Figure 1c,d) (the ND denotes a normal direction to the sample surface that was subjected to the cavitation test).

A reverse situation was observed in X6CrAl13 ferritic steel i.e. the perpendicular cut off sample showed

R. Jasionowski – Institute of Basic Technical Sciences, Maritime University of Szczecin, Szczecin, Poland
W. Polkowski, D. Zasada – Faculty of Advanced Technology and Chemistry, Military University of Technology, Warsaw, Poland

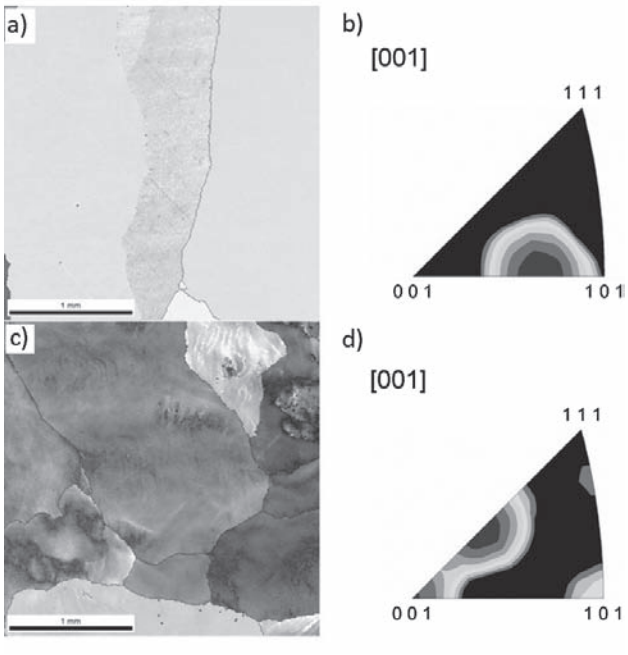

Figure 1 Results of the Electron backscatter diffraction (EBSD) analysis of the investigated X8CrNi25-21 steel: a) the inverse pole figure map and b) the inverse pole figure for the normal direction taken from the perpendicular cut off sample c) the inverse pole figure map d) the inverse pole figure for the normal direction taken from the parallel cut off sample.

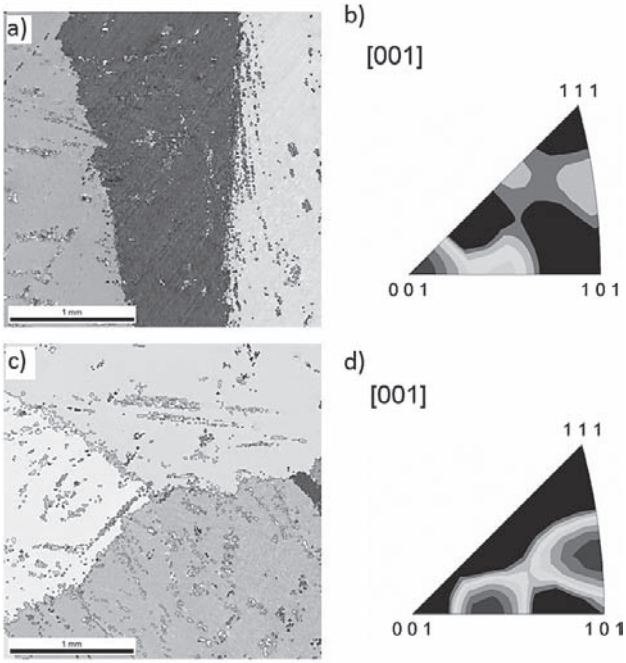

Figure 2 Results of the Electron backscatter diffraction (EBSD) analysis of the investigated X6CrAl13 steel: a) the inverse pole figure map and b) the inverse pole figure for the normal direction taken from the perpendicular cut off sample c) the inverse pole figure map d) the inverse pole figure for the normal direction taken from the parallel cut off sample.

the < 100 >// ND texture (Figure 2a,b) and the parallel cut off one had the < 110 >// ND texture (Figure 2c, d).

The examination of cavitational erosion was carried out on a jet-impact device [6]. Examinated samples had cylindrical shape with 20 mm diameter and 6 $^{\pm 0,5}$ mm height. Surface roughness of samples, measured by PGM-1C profilometer, was in range of 0,010 ÷ 0,015 μm. The samples were vertically mounted in rotor arms, parallel to the axis of water stream pumped continuously at 0,06 MPa through a 10 mm diameter nozzle located 1,6 mm away from the sample edge. The rotating samples were hitting by the water stream. Water flow of 1,55 m^3/h was constant during entire experiment.

The samples were examined up to 600 minutes. After 15, 30, 60, 90, 120, 180, 240, 360, 480 and 600 minutes samples were taken out from rotor arms, degreased in an ultrasonic cleaner for 10 minutes at 30 °C, dried in a laboratory drier for 15 minutes at 120 °C and finally weighted as well as observed on microscope. After that, specimens were mounted again in the rotor arms with maintaining their initial position in relation to the water stream.

The structural characterization of the investigated steels in its initial state and after cavitation tests was carried out by using FEI Quanta 3D field emission gun scanning electron microscopy FEG (SEM), EBSD system coupled with an electron backscatter diffraction (EBSD) system. For each sample the area of 1 200 x 1 200 μm was scanned with 6 μm step size. Acquired diffraction data was then analyzed with TSL OIM Analysis 5 commercial software.

STUDY RESULTS AND DISCUSSION

It was found that X8CrNi25-21 austenitic steel samples show a similar destruction mechanism independent on their preferred orientation (< 100 >// ND or < 110 >// ND). In both samples the destruction process starts with a plastic deformation, that is reflected by a formation of slip bands (Figure 3a).

The cracking initiated at grain boundaries areas. Moreover, the course of cavitation destruction was also strongly affected by a presence of non-metallic inclusions (namely manganese sulphide and aluminum oxide particles) leading to a presence a number of cavitation pits at the surface followed by a loss of whole grains upon a final stage of the process (Figure 3b). This detachment of whole grains in the austenitic steel is closely related to a fatigue nature of the cavitation destruction.

The X6CrAl13 ferritic steel with < 100 >// ND or < 110 >// ND texture was characterized by two following features: a very large grain size of 6 mm; and a presence of chromium enriched precipitates. It was found that these aforementioned features play a key role in the cavitational destruction mechanism. Effects of plastic straining and single small cavities formed in chromium enriched particles zones, were observed as first signs of the cavitational damage. A multiple action of the water stream on the samples surface results with a detachement of whole grains and conglomerates as well as with an increased surface roughness (Figure 4a,b).

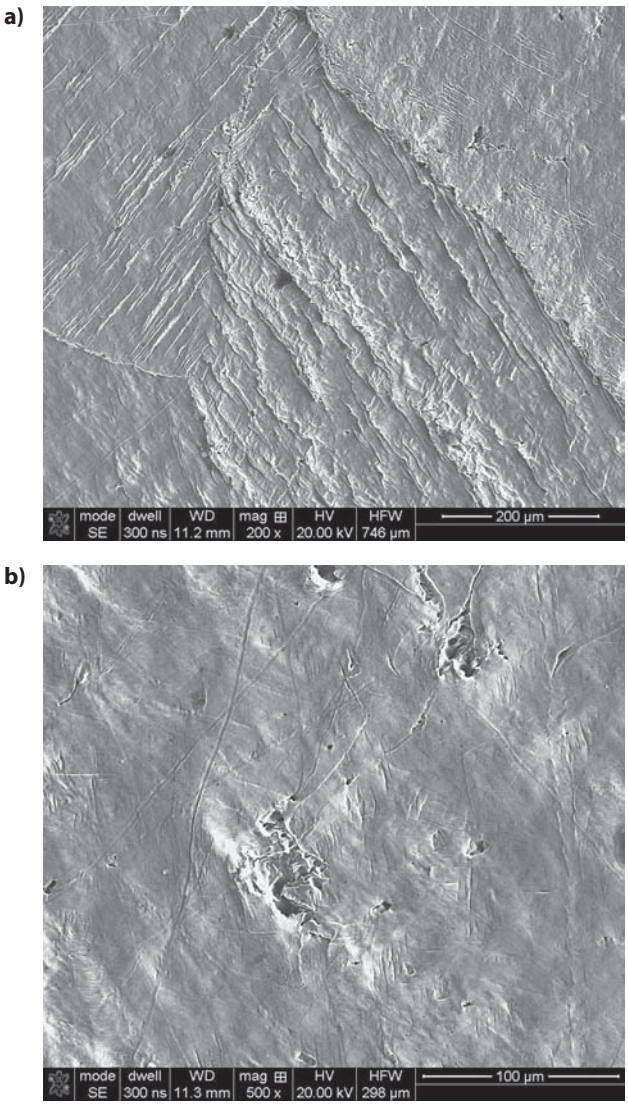

Figure 3 Cavitation wear of the X8CrNi25-21 austenitic steel a) the slip bands, b) cavitation pits at the surface.

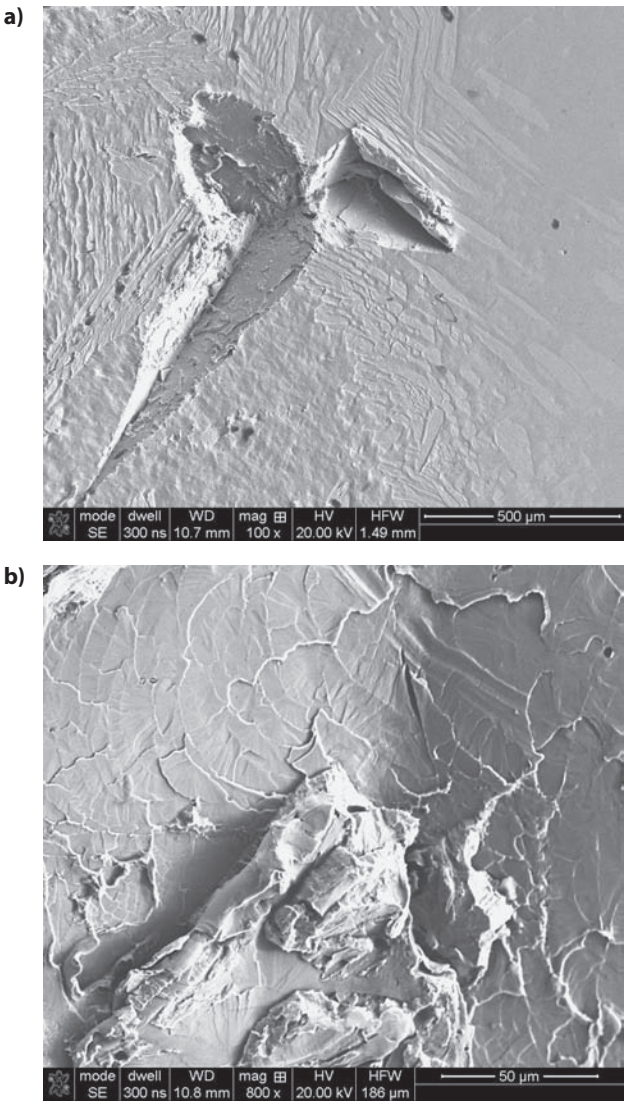

Figure 4 Cavitation wear of the X6CrAl13 ferritic steel a) loss of part of grains, b) visible fatigue striations.

The results of conducted cavitation test on the jet impact stand were plotted as mass loss vs. exposure time (Figure 5).

SUMMARY

Based on the results of conducted research on the effect of crystallographic texture on the cavitation resistance of as cast X8CrNi25-21 and X6CrAl13 steels have revealed:

- a better cavitation resistance of X8CrNi25-21 austenitic steel as compared to X6CrAl13 ferritic steel originating from its initially higher hardness (219 HV and 171 HV, respectively);
- a better cavitation resistance of both steels with the < 110 >// ND texture than their counterparts showing the < 100 > texture;
- a fatigue nature of the cavitation destruction. In both investigated steel the process starts with a plastic straining that is reflected by the formation of slip bands.

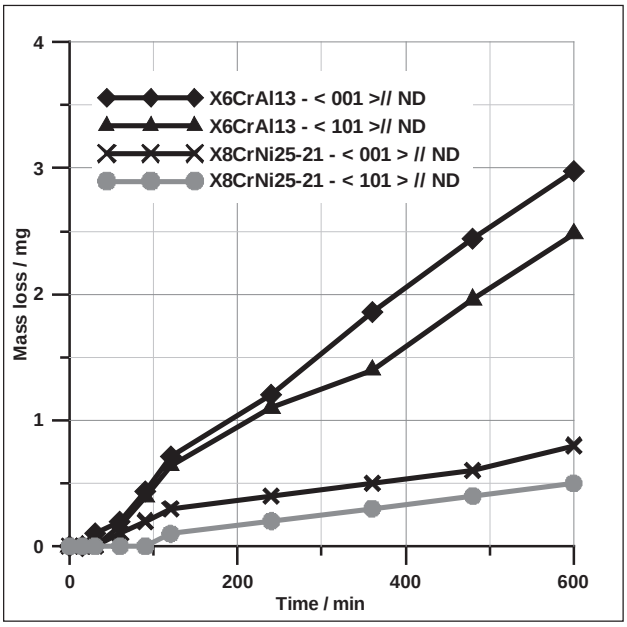

Figure 5 Mass loss vs. exposition time plots obtained for X8CrNi25-21 and X6CrAl13 steels in various structural states

Acknowledgements

Scientific work partly funded by the Polish Ministry of Education and Science in the years 2011 ÷ 2014 as a research project No. N N507 231 040.

REFERENCES

[1] H.R. Wenk, P. Van Houtte, Texture and anisotropy, Reports on Progress in Physics 67 (2004) 1367–1428.

[2] O. Engler, V. Randle, Introduction to Texture Analysis: Macrotexture, Microtexture, and Orientation Mapping, Second Edition (2009) CRC Press.

[3] U.F. Kocks, C.N. Tomé, H.R. Wenk, H. Mecking, Texture and Anisotropy: Preferred Orientations in Polycrystals and their effects on Materials Properties (2000) Cambridge University Press.

[4] G. Barnocky, R.H. Davis, Elastohydrodynamic collision and rebound of spheres: experimental verification, Physics of Fluids 31 (1988) 1324-1329.

[5] S.L. Ceccio, C.E. Brennen, Observations of the dynamics and acoustics of travelling bubble cavitation, Journal of Fluid Mechanics 233 (1991) 633-660.

[6] R. Jasionowski, D. Zasada, W. Polkowski, Destruction Mechanism of Z10400 Zn-based Alloy Subjected to Cavitational Erosion, Archives of Foundry Engineering 13 (2013) 48-52.

Note: The responsible translator for English language is W. Wisniewski, Szczecin, Poland